DiVA
http://www.diva-portal.org

Postprint

This is the accepted version of a paper presented at *Electronic Components and Technology Conference. Lake Buena Vista, FL. 31 May 2011 - 3 June 2011.*

Citation for the original published paper:

Xie, L., Shen, J., Mao, J., Jonsson, F., Zheng, L. (2011)
Co-design of flip chip interconnection with anisotropic conductive adhesives and inkjet-printed circuits for paper-based RFID tags.
In: *2011 61st Electronic Components and Technology Conference, ECTC 2011* (pp. 1752-1757).
Electronic Components and Technology Conference
http://dx.doi.org/10.1109/ECTC.2011.5898749

N.B. When citing this work, cite the original published paper.

Permanent link to this version:
http://urn.kb.se/resolve?urn=urn:nbn:se:kth:diva-49208

Co-Design of Flip Chip Interconnection with Anisotropic Conductive Adhesives and Inkjet-printed Circuits for Paper-Based RFID Tags

Li Xie, Jue Shen, Jia Mao, Fredrik Jonsson, and Lirong Zheng
iPack Vinn Excellence Center
School of Information and Communication Technology
KTH (Royal Institute of Technology)
Forum 120, 164 40 Stockholm-Kista, Sweden
Email: lixi@kth.se

Abstract

In this paper we study the radio frequency performance of interconnect using anisotropic conductive film (ACF). A series of experiments are conducted in order to measure and model the electrical characteristics of inkjet-printed circuits on paper substrate as well as the impedance parameters of ACF interconnect at high frequency. Four-point measurement structure, time domain reflectometry (TDR), vector network analyzer (VNA) and de-embedded technology are used to ensure the accuracy of experiments. Equivalent circuit models are built based on the experimental results. Finally, these models are considered as parts of the matching network and circuit design for the RFID receiver, which can be co-designed for developing paper-based electronic systems. It is found that since the difference between RFID tags with and without ACF interconnects is negligible, the influence of ACF interconnects can be ignored for paper-based UHF RFID tag. ACF is a feasible interconnect material for paper-based RFID tags.

1. Introduction

Radio-frequency identification (RFID) systems are today commonly used in applications such as product tracking, logistics, transport and storage. Driven by the increasing demands for low-cost, flexible, and environment-friendly RFID systems, paper, as one of the best and cheapest organic-substrate candidates, attracts more and more attention of researchers [1] [2]. Compared with other substrates such as FR4, paper has several advantages. It is biodegradable and could undergo high-efficiency reel-to-reel process, which means it can be used for mass production at low-cost [1]. Inkjet printing, as an efficient direct-write printing method, can be used to print electronics on paper substrates [2].

However, the relatively poor radio performance of printed circuits compared with circuits manufactured using conventional methods brings new challenges to integration technologies. First, paper can only stand temperature less than 120°C, which makes it impossible to apply traditional solder bonding technology. Second, paper is soft and fragile, so that it cannot bear high pressure. Third, the conductivity of inkjet-printed circuits is not as good as traditional circuits. All these challenges require new integration technologies for paper-based electronic systems.

As a new easy-handling bonding material for flip-chip interconnects, *anisotropic conductive adhesive* (ACA) has become a promising technology. ACA has two different forms: *anisotropic conductive* paste and *anisotropic conductive* film. *Anisotropic conductive film* (ACF) has been commonly used in paper-based RFID applications because of its advantages. It is non-sticky before bonding, which makes it easily to place and non-spreadable after bonding. Moreover, it can be cut into special shapes which can reduce waste. ACF realizes its Z-axis direction electrical conductivity through the conductive balls. Because ACF only conducts in one direction, the pitch between two adjacent pins or pads can be tens of um, which is determined by the size of conductive particles. One-direction-conductivity of ACF can also simplify the bonding process, since the short-circuit phenomenon caused by operation errors can be avoided.

Previous works on measuring the impedance parameters and mechanical characteristics of ACF interconnect have focused on traditional PCB board systems [3] [4] [5] [6]. In [3], the authors measured and compared the resistance, inductance and capacitance of two types of ACF flip-chip interconnects using the Ni-filled ball and Au-coated polymer ball. Ryu et al. [4] introduced the high-frequency SPICE models of those two kinds of ACFs. The S-parameter measurement and genetic algorithm were utilized for the extraction of the equivalent circuit parameters. In [5] [6], high frequency performance of several flip chip interconnects using anisotropic conductive adhesives were evaluated and compared. Furthermore, the characteristics and circuit models of inkjet-printed coplanar waveguides on quartz glass substrate have also been investigated in [7] [8]. According to [11], the performance of non-solder interconnects highly depends on the application environments, such as adhesives, surface pad finishes, bump materials and joint location. Due to the different electrical and mechanical properties of printed substrates, these results cannot be directly used on paper-based systems. It is essential to study the characteristics and performance of ACF interconnects on paper substrate.

In this paper we investigate the radio frequency properties of ACF interconnect and analyze the feasibility of ACF as interconnect material in paper-based RFID systems. We firstly conduct a series of experiments to measure the electrical properties of paper-based inkjet-printed lines, microstrip lines and the ACF interconnects. Then we build the electrical circuit models according to the measurement results. Based on the experiments and circuit models, we design the RFID tag to show a methodology of co-design in paper-based RFID tags, and we compare the difference of performance between tags with and without ACF interconnect.

The remaining of this paper is organized as follows. Section 2 contains experiments and measurement results. Based on the results and analysis, the co-design of RFID tag is applied and the influence of ACF interconnect are discussed at the end of this section. Finally this paper is summarized in section 3.

2. Experiments and measurements

In inkjet-printed paper-based electronic systems, the performance is influenced by material and process, such as the conductive ink, printing dot size, curing temperature and time. Hence, there is no existing accurate parameter of electrical characteristics, such as dielectric constant and conductivity. However, it is necessary to obtain such characteristics of paper substrate before circuit implementation. We therefore perform experiments to measure these parameters which can provide guidelines for circuit design.

DC resistance measurement is applied to test the sheet resistor of printed lines, by which we can calculate the conductivity. TDR measurement of printed microstrip line is implemented to obtain the dielectric constant.

The structure of a passive RFID tag is shown in Figure 1. A matching network is designed in order to conjugate-match equivalent impedance of the RFID tag IC and antenna.

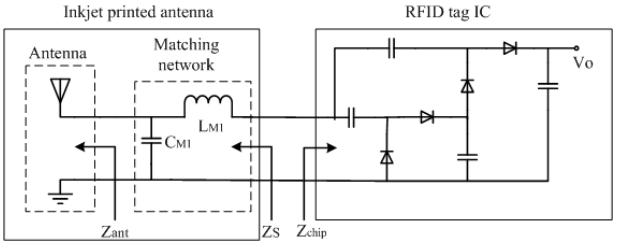

Figure 1. RFID tag structure

For paper-based systems, antenna pattern and matching network are inkjet-printed on paper. Tag IC is integrated on printed structure by ACF interconnects. Since the tag IC is serially connected with two ACF interconnects in such structure, the total impedance that antenna should match is the sum of the IC and two interconnects. The structure of a tag with ACF is shown in figure 2.

The equivalent circuit model of an ACF interconnect can be built based on its DC resistance and S-parameters. 4-point probe structure is used to measure the DC resistance of ACF interconnect. Its S-parameters can be obtained in two steps. First, we measure the S-parameters of the test device consisting of two transmission lines, a resistor and ACF interconnects. Then, the electrical parameters of ACF interconnects are extracted based on the de-embedding technology.

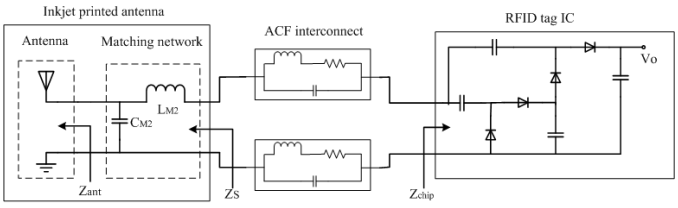

Figure 2. RFID tag with ACF interconnect

Using an equivalent circuit model, we calculate and compare the power transfer coefficient of RFID tag with and without ACF interconnect. From this we can have numerical impression of the influence of the ACF interconnect.

2.1. Material and manufacturing process

2.1.1 Material selection

HP Advanced Photo Paper is used as substrate. Although it is not as common, cheap and flexible as ordinary paper, it has smooth surface, great water and smudge resistance as it is coated, and it can stand high temperature.

For the conductors we use Cabot Conductive Ink-CCI-300 [9] as the inkjet-printed ink. The approximately electrical characters are listed in Table 1 according to the previous work. These values are influenced by actual experiment environment and setup. Therefore, we need to adjust them according to measurement results.

Table 1. Proposed electrical characteristics

Thickness of paper	Dielectric Constant	Thickness of ink	Loss Tangent	Conductivity
280um	2.8	0.5um/layer	0.002	3MS/m

Because the paper cannot stand long time temperature beyond 120°C, we use Anisotropic Conductive Film (ACF) 9703 from 3M Company [10] as the interconnection material. The film is applied between 15-70°C under low pressure of 15 psi.

We use conductive pen CM2200dMTP [12] as conductive material to form the ground of microstrip line.

2.1.2 Test device manufacture

In order to get electrical properties of paper-based inkjet-printed circuits and extract the parameters of ACF interconnect, we design a serial of microstrip line patterns as shown in Figure 3.

Figure 3. Pattern of samples

We can consider A2 as two cascaded A1, A3 as two cascaded A1, two ACF interconnects and a 0.3 Ω resistor. After comparing the different performance between A1, A2, and A3, we can obtain the parameters of the ACF interconnect as described in 2.2.3. The geometries of two groups of printed strips are listed in Table 2.

The fabrication of these microstrip samples includes three steps:

a). Print the test patterns on photo paper substrate using inkjet printer DMP-2800. In order to get good resolution and conductivity, we set the dimension of droplets to be 20um, and print three layers per pattern. In order to improve stability and performance, the samples are cured at 110°C for 30 minutes after printed.

Table 2. Geometries of printed strips

Patterns	L/(cm)	Ws/(um)	t/(um)
A1	4	200	1.5
A2	8	200	1.5
A3	4.1+4.1with interval of 0.1	200	1.5

b). Paint the backside of paper substrate by conductive pen as the ground, to form microstrip lines. The width of ground is 4-5 times as the width of printed strips. For speed reason, in production, coplanar waveguide or aluminum coated paper could be used.

c). Bond two strips in A3 by a 0Ω resistor (the real value is 0.3Ω according to the measurement result) using ACF.

The ACF bonding can be applied manually by hand. The bonding process is shown in Figure 4.

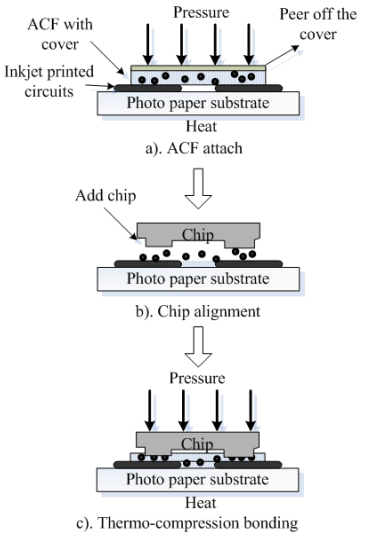

Figure 4. ACF bonding process

2.2. Experiment design and results

2.2.1. DC resistance measurement

In order to get rid of the influence of the test instruments, we apply 4-point probe to measure the DC resistance of interconnects and sheet resistor of inkjet-printed wires.

a) Sheet resistance and conductivity measurement

The structure shown in Figure 5 can be used to measure the sheet resistance of inkjet-printed line, $R_{\square}$.

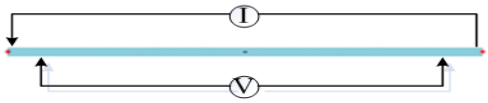

Figure 5. 4-point probe structure for sheet resistance

According to Equation 2, $R_{\square}$ can be computed as long as the length L and the width W of the printed line are known.

$$R = R_{\square} * L/W \quad (1)$$

Here we have L = 70mm, W = 2mm, and set I = 1mA. We can measure the values V = 10.5mV, R = 10.5 Ω. According to Equation (1), $R_{\square}$ = 0.3Ω.

The thickness of the printed lines is 1.5um. Using the following equation, we can obtain the value of conductivity σ to be 2.2MS/m, which is different from the value in Table 1.

$$\rho = R_{\square}/t = 0.3\Omega/1.5\mu m \quad (2)$$

$$\sigma = 1/\rho = 2.2\ MS/m \quad (3)$$

b) Resistance of ACF interconnect measurement

We use the following patterns for the interconnect measurement. The width of lines is 1mm. After both Up (Figure 6.a) and Bottom (Figure 6.b) structure are printed on paper substrate using inkjet printer, they are bonded together by ACF as the structure showed in Fig 6.c. The width of lines in both Up and Down is 1mm, giving a total area of the ACF interconnect of 1mm^2.

A constant current I is added between port 1 and 2, which would pass through interconnect marked by black circle in Figure 6.c. By measuring the voltage V between port 3 and 4, we can calculate the DC resistance R of the ACF interconnect.

In the experiment, we choose I = 10mA. The measured voltage V = 2.6mV. So the DC resistance of a 1mm^2 ACF interconnect is, R = V/I = 0.26Ω.

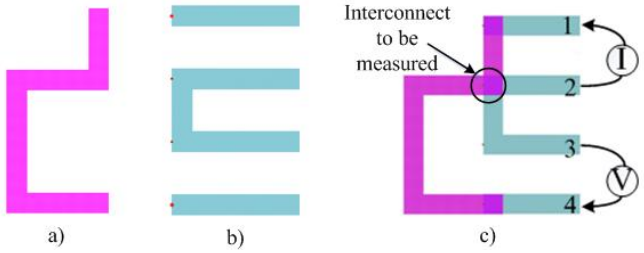

Figure 6. Four-point measurement for interconnect a) Up b) Bottom c) test setup

2.2.2. Time domain measurement

In order to obtain the properties of paper substrate and to have a direct impression of the influence of the ACF interconnect, we conduct TDR measurement. The TDR diagram is shown in Figure 7 [8]. 50Ω SMA cable with the length of 1.5 meter is connected between TDR instrument and the microstrip line. The characteristic impedance and propagation delay of microstrip line samples can be obtained by the TDR measurement. Therefore, we can obtain the dielectric constant of inkjet-printed lines on paper substrate. After comparing the difference between sample A2 and A3, we can have a preliminary impression of the influence of ACF interconnects.

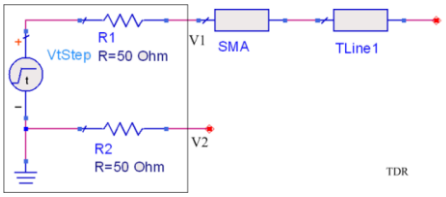

Figure 7. TDR block diagram

a) Electrical properties of paper substrate

The measurement results of TDR and the rising edge results are shown in Figure 8 and Figure 9, respectively. From these figures, we can see the rise time of the incident step is 120ps. Due to the delay caused by the SMA cable, the rise time is further increased to 200ps. When A2 is connected, the propagation delay is approximately 450ps, which is much bigger than half of the rise time (100ps) in this setup. Therefore, it is reasonable to model the samples as transmission lines.

The *propagation delay* (PD) of microstrip line A2 is 450ps. According to Equation 4 and 5, we can calculate the value of electrical property as 2.85, which is slightly different from our assumed value.

$$v_p = \frac{L}{PD} = \frac{0.08m}{450ps} \quad (4)$$

$$\varepsilon_r = \left(\frac{c}{v_p}\right)^2 = \left(\frac{3 \times 10^8}{0.08/(450 \times 10^{-12})}\right)^2 = 2.85 \quad (5)$$

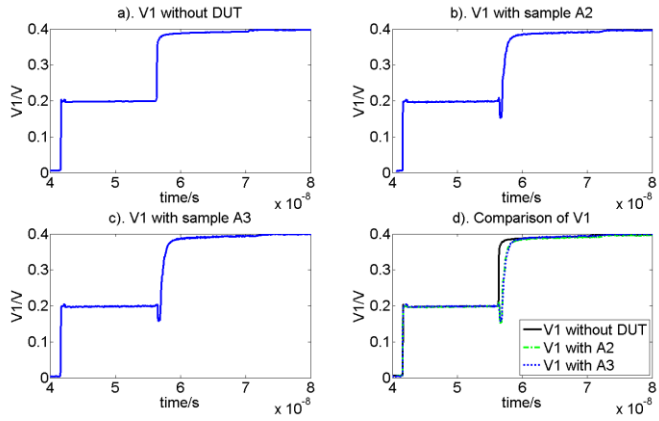

Figure 8. TDR measurement results

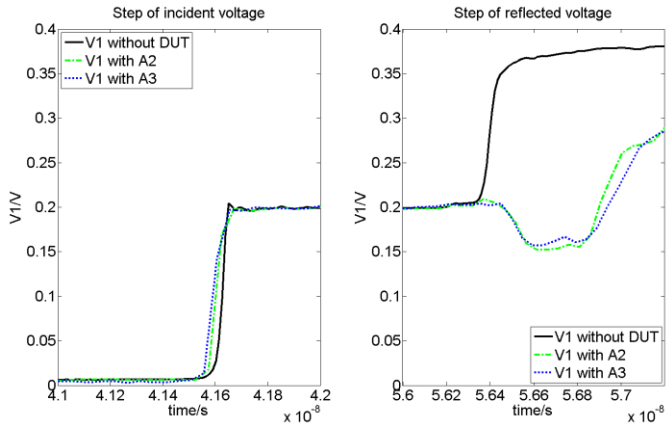

Figure 9. Rising edge in TDR measurement results

b) Influence of ACF interconnect

From Figure 8, we could see that the incident voltage is 0.2V, and the voltage reflected by microstrip line A2 is 0.155V-0.2V=-0.045V. With the following equations, we can derive the characteristic impedance of microstrip A2, which equals to 31.6 Ω.

$$\rho = \frac{Vr}{V1} = \frac{0.045}{0.2} = -0.225 \quad (6)$$

$$\rho = \frac{Zt - Z0}{Zt + Z0} = \frac{Zt - 50}{Zt + 50} \quad (7)$$

Under the same way, we could obtain that the characteristic impedance of A3 is 33.3 Ω, which is slightly bigger than A2. This is mainly caused by two ACF interconnects and a resistor in A3.

From the TDR result, we can also see that the influence of the ACF interconnect to the reflected voltage is not significant. The rise time of 450ps also indicates that the frequency response is sufficient to transmit UHF signals by paper-based inkjet-printed lines and ACF interconnect.

2.2.3. Frequency domain measurement

a) Electrical characteristics verification

In order to verify the measured and calculated electrical characteristics, we simulate the S-parameters of transmission lines (sample A1 and sample A2) in Advanced Design System (ADS) using updated electrical characteristics listed in Table 3.

Table 3. Electrical characters used in ADS simulation

Thickness of paper	Dielectric Constant	Thickness of ink	Loss Tangent	Conductivity
280um	2.85	1.5um	0.002	2.2MS/m

The simulation results and measured results are compared in Figure 10, from which we can see that the results match quite well in most of the frequency ranges. The mis-match may be caused by the parasitic impedance between the SMA and the transmission line.

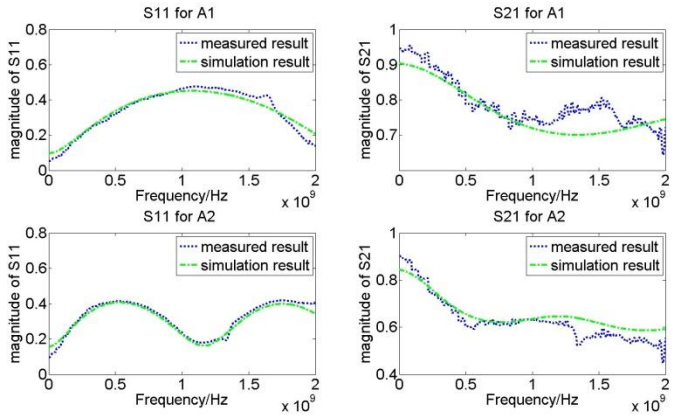

Figure 10. Comparison of simulated and measured S-parameters for sample A1 and sample A2

The good agreement between measurement and simulation results indicates that we can safely rely on these parameters while we design pattern of printed lines, the printed antenna and do simulation of the whole circuit.

b) De-embedding procedure of the ACF interconnect

In order to get the parameters of the interconnect, we choose the following de-embeding procedure as shown in Figure 11.

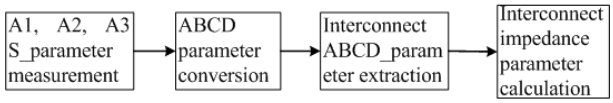

Figure 11. Procedure for interconnect parameter

Agilent 8755ES S-parameter Vector Network Analyzer (VNA) is used to measure the S-parameters of samples for the frequency band between 200KHz and 2GHz. Based on the

equations (8)-(12), S-parameters can be converted into ABCD-parameters [8].

$$\Delta S = S_{11}S_{22} - S_{12}S_{21} \quad (8)$$
$$A = (1 + S_{11} - S_{22} - \Delta S)/(2S_{21}) \quad (9)$$
$$B = (1 + S_{11} + S_{22} + \Delta S)Z_r/(2S_{21}) \quad (10)$$
$$C = (1 - S_{11} - S_{22} + \Delta S)(2S_{21}Z_r) \quad (11)$$
$$D = (1 - S_{11} + S_{22} - \Delta S)(2S_{21}) \quad (12)$$

The ABCD-parameters of 4cm microstrip line (sample A1) are A1 B1 C1 and D1, respectively the ACF interconnects together with 0.3Ω resistor are Aa Ba Ca and Da, of the sample A3 are A3 B3 C3 and D3. Assume the ground impedance is negligible, the parameters of microstrip line in A1 are the almost same with two microstrip lines in A3, and quasi-transverse electromagnetic (TEM) wave is transformed through the whole device. Hence, sample A3 can be regarded as the cascading of sample A1, ACF and A1. Therefore, we can calculate the values of Aa, Ba, Ca, and Da by Equation 13.

$$\begin{bmatrix} Aa & Ba \\ Ca & Da \end{bmatrix} = \begin{bmatrix} A1 & B1 \\ C1 & D1 \end{bmatrix}^{-1} \begin{bmatrix} A3 & B3 \\ C3 & D3 \end{bmatrix} \begin{bmatrix} A1 & B1 \\ C1 & D1 \end{bmatrix}^{-1} \quad (13)$$

According to [3], ACF interconnect can be represented by the circuit model as shown in Figure 12.a. Therefore, sample A3 can be represented by the circuit model in Figure 12.b. Consequently, we can calculate the values of La and Ca through the following equations:

$$\begin{bmatrix} Aa & Ba \\ Ca & Da \end{bmatrix} = \begin{bmatrix} 1 & Z \\ 0 & 1 \end{bmatrix} \quad (14)$$
$$Z = Za + R0 + Za \quad (15)$$
$$Ya = 1/Za = jwCa + (1/(jwLa + Ra)) \quad (16)$$

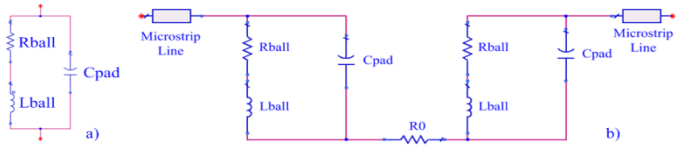

Figure 12. Equivalent circuit model of a). ACF interconnect b). Sample A3

Notice that the values of La, Ca, Ra and R0 are normalized values in the equations. We need to replace them by actual values. The final L_{ball} and C_{pad} are showed in Figure 13.

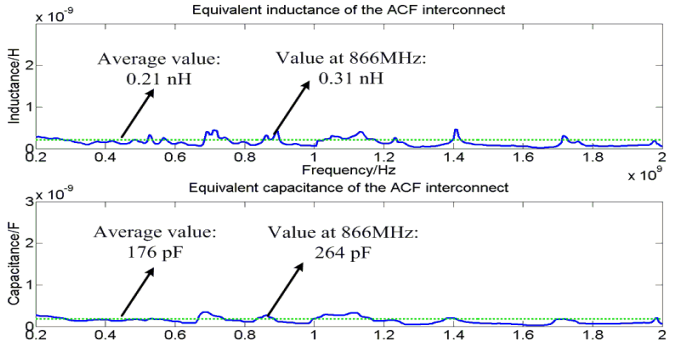

Figure 13. Inductance and capacitance of ACF interconnect

According to the calculation, we can get the average values: L_{ball} = 0.21nH, C_{pad} = 176pF, R_{ball} = 0.26Ω. Because the pad size, the material of the pad and the substrate are different, the values of equivalent parameters are different from the measurement results in [4].

Notice that the curves are not smooth. The reason for this is that the parameters of interconnects are very small compared with transmission lines. As a result the de-embedding process makes the results sensitive. A more accurate model could be obtained using more precise de-embedding structure, but since the influence of the ACF is so small and other parts of the circuit (such as the transmission line) will have more influence, this is in most cases not necessary.

2.3. Co-design concept and influence analysis

2.3.1. Co-design concept of the antenna, matching network, ACF interconnect and tag IC

As long as equivalent circuit models are extracted, we could take them into consideration while performing paper-based RFID tag design. We exemplify the co-design concept through a dipole antenna and an 866MHz UHF IC. The equivalent circuit models together with the example values are shown in Figure 14.

Suppose $Z_{ant} = R_{ant} + jX_{ant}$, $Z_{chip} = R_{chip} + jX_{chip}$. Let P_L denote the power that tag IC can receive. Let P_F denote the maximum power the tag could have received according to the Friis equation. Then the power transfer coefficient τ can be computed by,

$$\tau = \frac{P_L}{P_F} = \frac{4R_{chip}R_{ant}}{|Z_{ant} + Z_{chip}|^2} \quad (17)$$

When the antenna and IC are conjugate-matched ($R_S = R_{chip}$, $X_S = -X_{chip}$), τ is maximized to 1. It means that the RFID tag IC can absorb all the power delivered by the antenna. Therefore, a matching network should be designed to adjust the load impedance $Z_S = R_S + jX_S$, so that it equals to the complex conjugate of the source impedance Z_{chip}.

In the following, we choose L matching network. Using Smith Chart, we can get L_{M1}=7.52nH, C_{M1}=1.83pF.

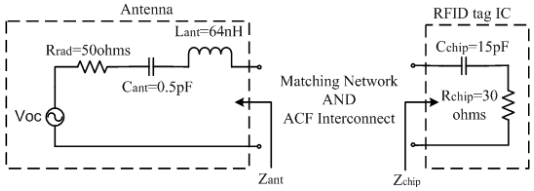

Figure 14. Equivalent circuit of RFID tag

2.3.2. ACF interconnect influence analysis

While we take ACF interconnect into consideration, the structure of the RFID tag is shown in Figure 2. The value of a ACF interconnect at the frequency of 866MHz is 0.31nH and 264pF, which provides equivalent impedance of 0.12 – 1.15j. The real impedance that RFID tag IC shows to the matching network shifts from 30-12.2j to 30.24-14.5j.

In order to get perfect match, we should use LM2 = 7.95nH and CM2 = 1.80pF, which are slightly different from previous values. While we conduct printed antenna and printed matching network design, we need to shift the pattern so as to fit the new values.

However, let us think back to the power transfer coefficient τ. If we consider the influence of ACF interconnects, the τ becomes,

$$\tau = \frac{4 \times 30 \times 30.24}{|(30 + 12.2j) + (30.24 - 14.5j)|^2} = 99.85\% \quad (17)$$

As the τ only changes 0.15%, the influence of ACF interconnect is safely to be ignored in most kinds of applications.

3. Conclusions

The electrical characteristics of photo paper substrate and inkjet-printed microstrip lines are measured during a series of experiments. Time domain reflectometry (TDR) measurement is applied to derive the dielectric constant and conductivity. The measured S-parameters are compared with those obtained from ADS simulation and show good agreement. The DC resistance of anisotropic conductive film (ACF) is measured by 4-point probe structure. De-embedding technology and extraction procedure are used to get high frequency properties of the ACF interconnect. Based on the measurement results, we extract the equivalent circuit model of the ACF interconnect.

A paper-based RFID tag system is designed as an example based on the equivalent circuit model. The matching network and the ACF interconnect together with the inkjet-printed antenna can be co-designed. However, since there only exists negligible difference of power transfer coefficient between RFID tags with and without ACF interconnects, the influence of ACF interconnects can be safely ignored for paper-based UHF RFID tag. ACF is a feasible material for paper-based RFID tags.

Acknowledgments

This work was financially supported by Vinnova (The Swedish Governmental Agency for Innovation Systems) through the Vinn Excellence centers program. The China Scholoarship Council (CSC) is acknowledged for providing study grant.

References

1. Vyas, R.; Lakafosis, V.; Rida, A.; Chaisilwattana, N.; Travis, S.; Pan, J.; Tentzeris, M.M.; , "Paper-Based RFID-Enabled Wireless Platforms for Sensing Applications," *IEEE Transactions on Microwave Theory and Techniques*, vol.57, no.5, pp.1370-1382, May 2009
2. Li Yang; Rida, A.; Vyas, R.; Tentzeris, M.M.; , "RFID Tag and RF Structures on a Paper Substrate Using Inkjet-Printing Technology," *IEEE Transactions on Microwave Theory and Techniques*, vol.55, no.12, pp.2894-2901, Dec. 2007
3. Seungyoung Ahn; Woonghwan Ryu; Myung-Jin Yim; Junho Lee; Young-Doo Jeon; Woopoung Kim; Kyung-Wook Paik; Joungho Kim; , "Over 10 GHz equivalent circuit model of ACF flip-chip interconnect using Ni-filled ball and Au-coated polymer balls," *Electronics Manufacturing Technology Symposium, 1999. Twenty-Fourth IEEE/CPMT* , vol.,
4. Woonghwan Ryu; Myung-Jin Yim; Seungyoung Ahn; Junho Lee; Woopoung Kim; Kyung-Wook Paik; Joungho Kim; , "High-frequency SPICE model of anisotropic conductive film flip-chip interconnections based on a genetic algorithm," *IEEE Transactions on Components and Packaging Technologies*, vol.23, no.3, pp.542-545, Sep 2000
5. Myung-Jin Yim; In ho Jung; Hyung-Kyu Choi; Kijoong Kim; Jia-Sang Hwang; Jin-Yong Ahn; Woonseong Kwon; Kyung Wook Paik; , "Flip chip interconnection using anisotropic conductive adhesives for RF and high frequency applications," *Electronic Components and Technology Conference, 2003. Proceedings. 53rd* , vol., no., pp. 1398- 1403, May 27-30, 2003
6. Myung Jin Yim; In Ho Jeong; Hyung-Kyu Choi; Jin-Sang Hwang; Jin-Yong Ahn; EWoonseong Kwon; Kyung-Wook Paik; , "Flip chip interconnection with anisotropic conductive adhesives for RF and high-frequency applications," *IEEE Transactions on Components and Packaging Technologies*, vol.28, no.4, pp. 789- 796, Dec. 2005
7. Botao Shao; Weerasekera, R.; Li-Rong Zheng; Ran Liu; Zapka, W.; Lindberg, P.; , "High Frequency Characterization of Inkjet Printed Coplanar Waveguides," *12th IEEE Workshop on Signal Propagation on Interconnects, SPI 2008.* vol., no., pp.1-4, 12-15 May 2008
8. Botao Shao; Weerasekera, R.; Woldegiorgis, A.T.; Li-Rong Zheng; Ran Liu; Zapka, W.; , "High frequency characterization and modelling of inkjet printed interconnects on flexible substrate for low-cost RFID applications," *Electronics System-Integration Technology Conference, 2008*, vol., no., pp.695-700, 1-4 Sept. 2008
9. http://www.cabot-corp.com/New-Product-Development/Printed-Electronics/Products
10. http://multimedia.3m.com/mws/mediawebserver?66666UuZjcFSLXTtnxfVMxz6EVuQEcuZgVs6EVs6E666666--
11. Lee, C.; Yeo, A.; Tan Ai Min; , "Flip Chip Interconnection Systems and its Reliability Performance," *Electronics Systemintegration Technology Conference, 2006.* vol.2, no., pp.1032-1039, 5-7 Sept. 2006
12. http://datasheet.octopart.com/CW2200MTP-CircuitWorks-datasheet-12789.pdf